ACS OMEGA

Open Access

http://pubs.acs.org/journal/acsodf

Article

Assembly-Driven Oxidative Degradation of Melarsomine Triggered by Cyanuric Acid

Dongjun Baek,[#] Nakyeong Kim,[#] Dahee Jung, Jeong Sook Ha, and Yongju Kim*

Cite This: *ACS Omega* 2024, 9, 30986−30992

Read Online

ACCESS | Metrics & More | Article Recommendations | Supporting Information

ABSTRACT: Molecular self-assembly can trigger or regulate specific chemical reactions that would otherwise be infeasible when molecules exist individually. Supramolecular structures can significantly affect the rate of chemical reactions; therefore, optimizing supramolecular structures by manipulating intermolecular interactions is crucial for achieving the desired reactivity. Melamine is known to form hydrogen bonds with cyanuric acid, resulting in the formation of a supramolecular network. Melarsomine, an effective medication for heartworm treatment in dogs, contains a melamine moiety. It has yet to be studied how the chemical stability of melarsomine is affected by its interaction with other molecules. Herein, we report the formation of a two-dimensional supramolecular network between melarsomine and cyanuric acid via hydrogen bonds. This network structure captures dissolved oxygen in an aqueous solution, accelerating the oxidative degradation of melarsomine.

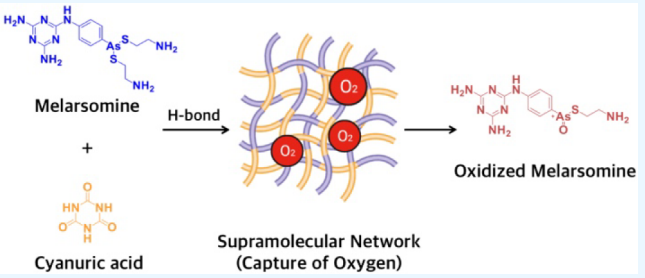

1. INTRODUCTION

Supramolecular chemistry explores the unique noncovalent interactions between molecules, such as hydrogen bonds, hydrophobic interactions, van der Waals forces, $\pi-\pi$ interactions, and ionic bonds.[1−4] Specific structures, including micelles, vesicles, sheets, networks, and ribbons, can be formed through the precise control of noncovalent interactions.[5−8] Combining multiple molecules results in supramolecules with novel and distinct functions not observed in individual molecules.[9,10] Among these functions, assembly-driven reactions involve initiating or controlling a particular chemical reaction by forming a supramolecule.[11] This approach enables the simple and efficient control of reactions without modification of other variables. For example, Jiang et al. assembled a monomer containing an azide and an alkyne into a nanofiber to induce a click reaction without using a metal catalyst.[12] Wang et al. fabricated vesicles composed of pyridine-based amphiphiles to induce nucleophilic aromatic substitution reactions through molecular assembly.[13] This demonstrates a correlation between the formation of supramolecular structures and the occurrence of chemical reactions.

Network structures have a greater tendency to undergo chemical reactions because of their large surface area, which provides numerous opportunities for chemical interactions and increases their susceptibility to such reactions.[14] Supramolecular networks can be formed by the interactions of molecular units through hydrogen bonds; as a result, they exhibit various structural and physical properties. For example, Zhang et al. reported that two-dimensional (2-D) hydrogen-bonded supramolecular networks can serve as templates for controlling chemical reactions.[15] These networks, with tunable cavities of different sizes and shapes, have been used as molecular templates for hosting and spatially confining reactions, demonstrating their control and predictability in chemical processes. Kimizuka et al. reported that melamine and cyanuric acid (CYA) form a unique type of hydrogen bond that results in the formation of a consecutive supramolecular network.[16] In aqueous environments, functionalized melamine and CYA form bilayer structures through hydrogen bonds, demonstrating the adaptability of these networks in various solvents. This intermolecular interaction involves the sharing of electrons between the nitrogen atoms of melamine and the nitrogen atoms of CYA, leading to the formation of a highly stable and organized structure.[17] Melarsomine, a derivative of melamine, is the primary component in Immiticide, a canine heartworm treatment. It is water-soluble and is absorbed by the body and muscles to eliminate heartworms.[18] It is important to note that drugs interact with various molecules, which can affect their chemical stability and physical properties.[19] However, the chemical instability of melarsomine after interaction with other molecules and the formation of supramolecular assemblies have not yet been studied.

Herein, we report a strategy for controlling the decomposition rate of melarsomine by creating a 2-D network structure using a

Received: May 3, 2024
Revised: June 10, 2024
Accepted: June 20, 2024
Published: July 1, 2024

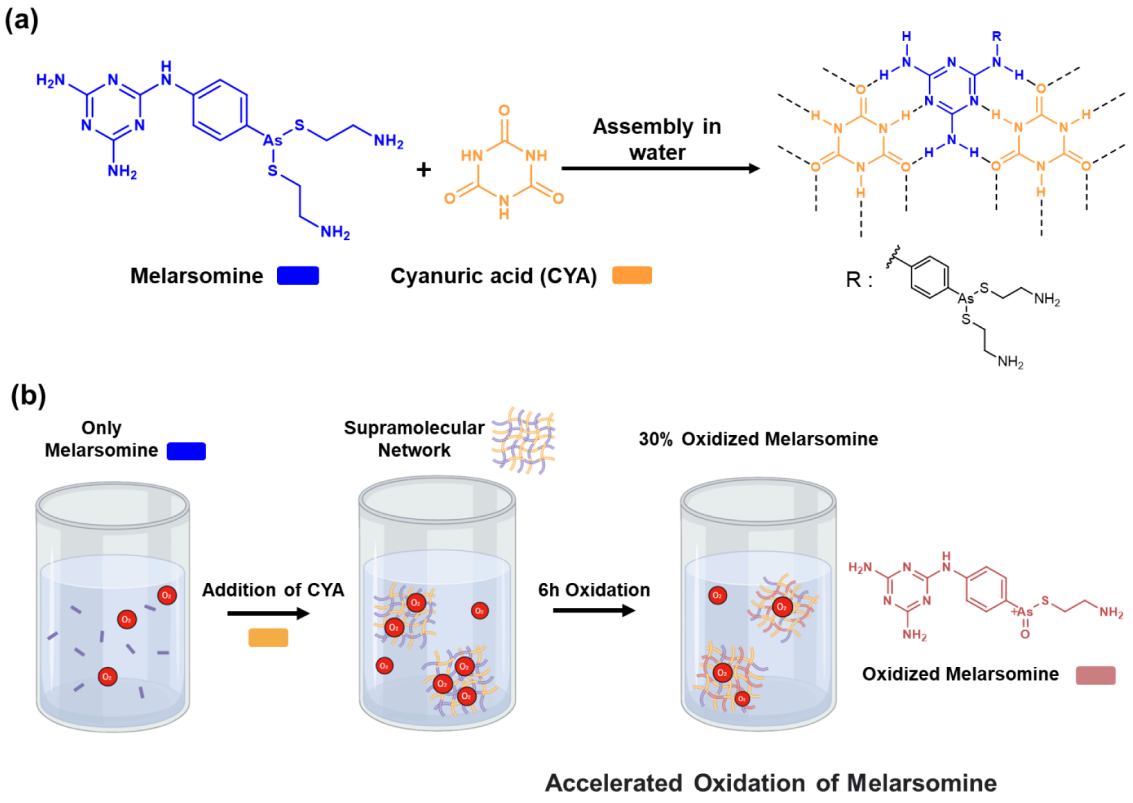

Figure 1. (a) Chemical structures of melarsomine and cyanuric acid (CYA) and the hydrogen-bonded network formed between them. (b) Schematic illustration of the accelerated oxidation of melarsomine by the supramolecular network created by the assembly of melarsomine and CYA.

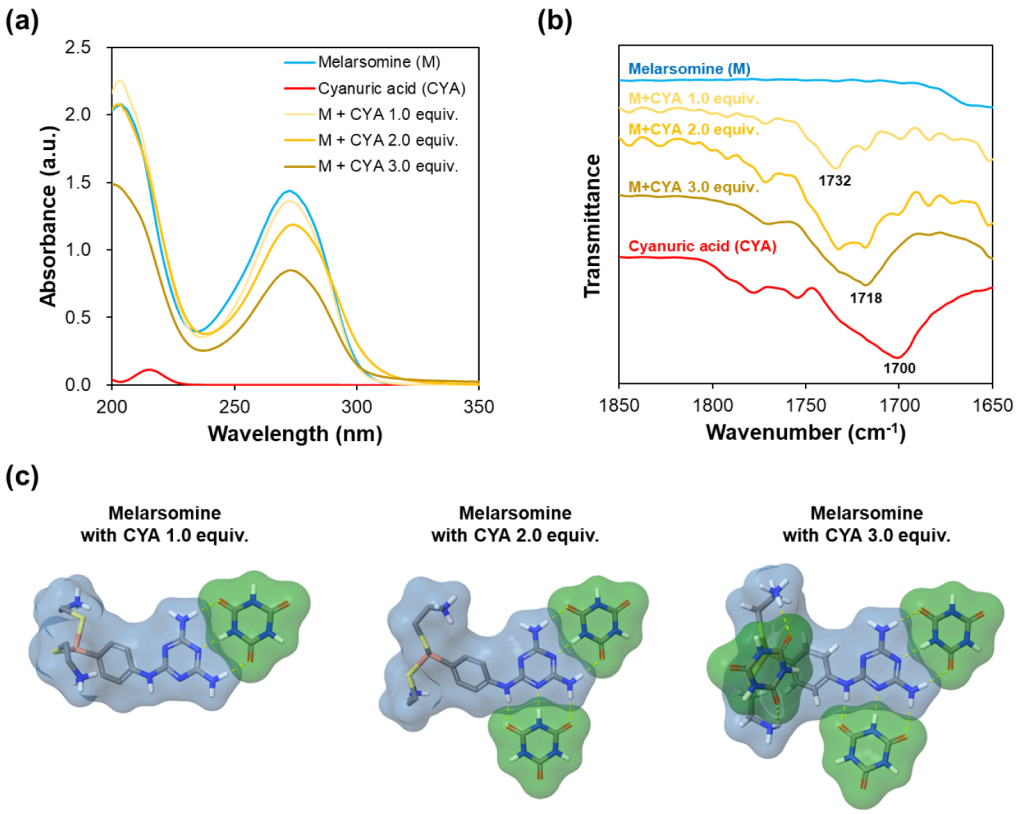

Figure 2. (a) Absorption spectra of melarsomine (M) (600 μM), cyanuric acid (CYA) (600 μM), and melarsomine with 1.0, 2.0, and 3.0 equiv of CYA added. (b) FT-IR spectra of melarsomine, CYA, and melarsomine with added 1.0, 2.0, and 3.0 equiv of CYA. (c) DFT calculations of the hydrogen bond sites in the supramolecular network formed by melarsomine and 1.0, 2.0, and 3.0 equiv of CYA.

https://doi.org/10.1021/acsomega.4c04247
ACS Omega 2024, 9, 30986−30992

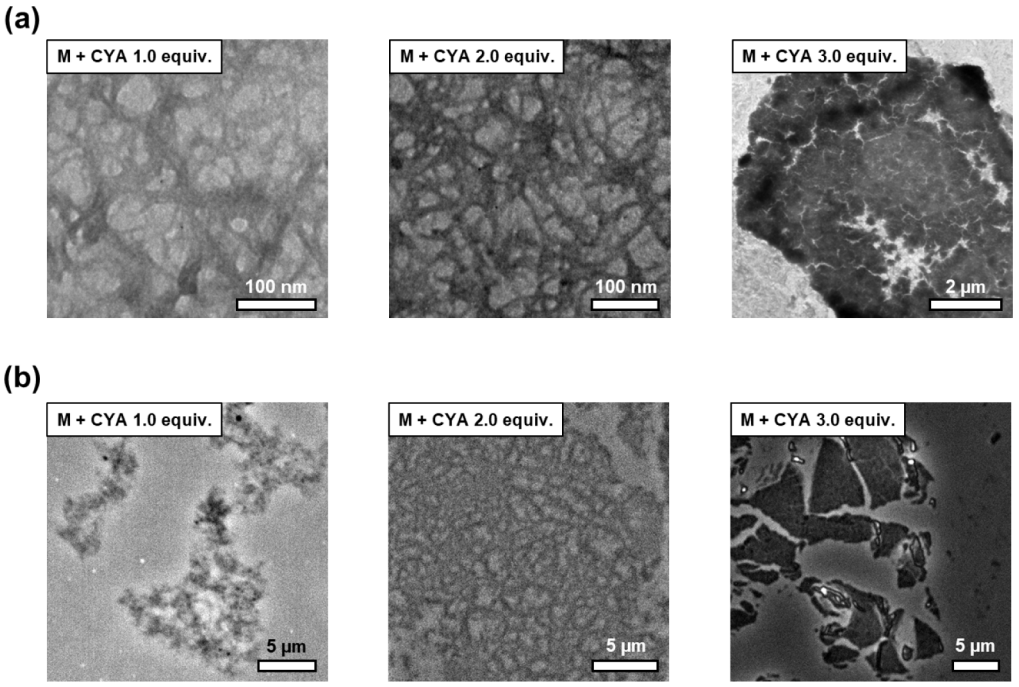

Figure 3. (a) TEM and (b) optical microscopy images of the assembled structures of melarsomine (600 μM) with different amounts of cyanuric acid (CYA).

supramolecular approach. When CYA was added to melarsomine, a network structure spanning several tens of micrometers was formed. This network structure was created by the formation of hydrogen bonds between the melamine moiety of melarsomine and CYA. This network captures ambient dissolved oxygen, which facilitates the oxidation and decomposition of melarsomines. This feature promotes efficient oxidative degradation by exposing drug molecules to oxygen.

2. RESULT AND DISCUSSION

2.1. Self-Assembled Structures of Melarsomine and Cyanuric Acid. Melarsomine contains a melamine moiety with a bis(2-aminoethyl) phenylarsonodithioite group (Figure 1a). Because of the high aqueous solubility of the several amino groups of melarsomine, no aggregates were observed in its transmission electron microscopy (TEM) image (Figure S1). Hydrogen bonds between melarsomine and CYA were utilized to endow melarsomine with self-assembling features.[20] Samples were prepared by adding different amounts of CYA to melarsomine, and the intermolecular interactions between them were studied by using UV−vis spectroscopy. The absorbance of melarsomine at 275 nm was initially measured to be 1.44 arbitrary units (AU), gradually decreasing to 1.35, 1.16, and 0.85 AU with the addition of 1.0 to 3.0 equiv of CYA. This represents a significant decrease in the absorption coefficient, indicating that the addition of CYA to melarsomine imparted aggregation properties (Figures 2a and S2).[21] Fourier transform infrared (FT-IR) spectroscopy was used to investigate whether CYA formed hydrogen bonds with melarsomine (Figure 2b). The complex of melarsomine and CYA exhibited a shift to lower wavenumbers at 1732 cm^{-1} and the emergence of new bands at 1718 cm^{-1}. These changes indicate variations in the carbonyl stretching vibrations of CYA due to hydrogen bond formation.[22] Proton nuclear magnetic resonance (^{1}H NMR) spectroscopy revealed that all hydrogen peaks of melarsomine shifted downfield upon the addition of 1.0 equiv of CYA, indicating the formation of hydrogen bonds between CYA and melarsomine (Figure S3).[23] However, no discernible additional shift occurred when more than 1.0 equiv of CYA was added. The hydrogen peak of the melamine moiety was not observed in the NMR spectra because of hydrogen−deuterium exchange in deuterium oxide (Figures S4 and S5). Density functional theory (DFT) calculations (B3LYP-D3 basis set) revealed the hydrogen bond sites between melarsomine and CYA. When 1.0 and 2.0 equiv of CYA were used, CYA formed hydrogen bonds with the melamine moiety of melarsomine. When 3.0 equiv of CYA was used, two CYA molecules formed hydrogen bonds with the melamine moiety, while one CYA molecule formed hydrogen bonds with the ammonium moiety of its aliphatic chain (Figures 2c and S6).

The supramolecular structures formed via hydrogen bonds between melarsomine and CYA were characterized by negatively stained TEM. Notably, CYA did not form aggregates because of its high solubility in aqueous solutions (Figures S7 and S8). The TEM images show sparse networks of the complex in aqueous solution, with a single-strand width of approximately 10 nm in the presence of 1.0 equiv of CYA. In the presence of 2.0 equiv of CYA, the networks appeared dense. In addition, dense networks resembling sheets were observed when 3.0 equiv of CYA was added to melarsomine (Figure 3a). Optical microscopy (OM) was used to study the assembled structures ofmelarsomine and CYA in solution. The OM images revealed that melarsomine and 1.0 equiv of CYA formed irregular aggregates, while 2.0 equiv of CYA formed networks with a length of approximately 20 μm. Sheet formation was observed upon the addition of 3.0 equiv of CYA. The sizes of the sheets ranged from 2 to 10 μm, indicating the significance of CYA concentration on their morphology (Figure 3b).

2.2. Oxidative Degradation of Melarsomine Driven by Supramolecular Structures. As many drugs are generally degraded by oxidation or hydrolysis for elimination from the body, the decomposition of melarsomine under oxidation

https://doi.org/10.1021/acsomega.4c04247
ACS Omega 2024, 9, 30986−30992

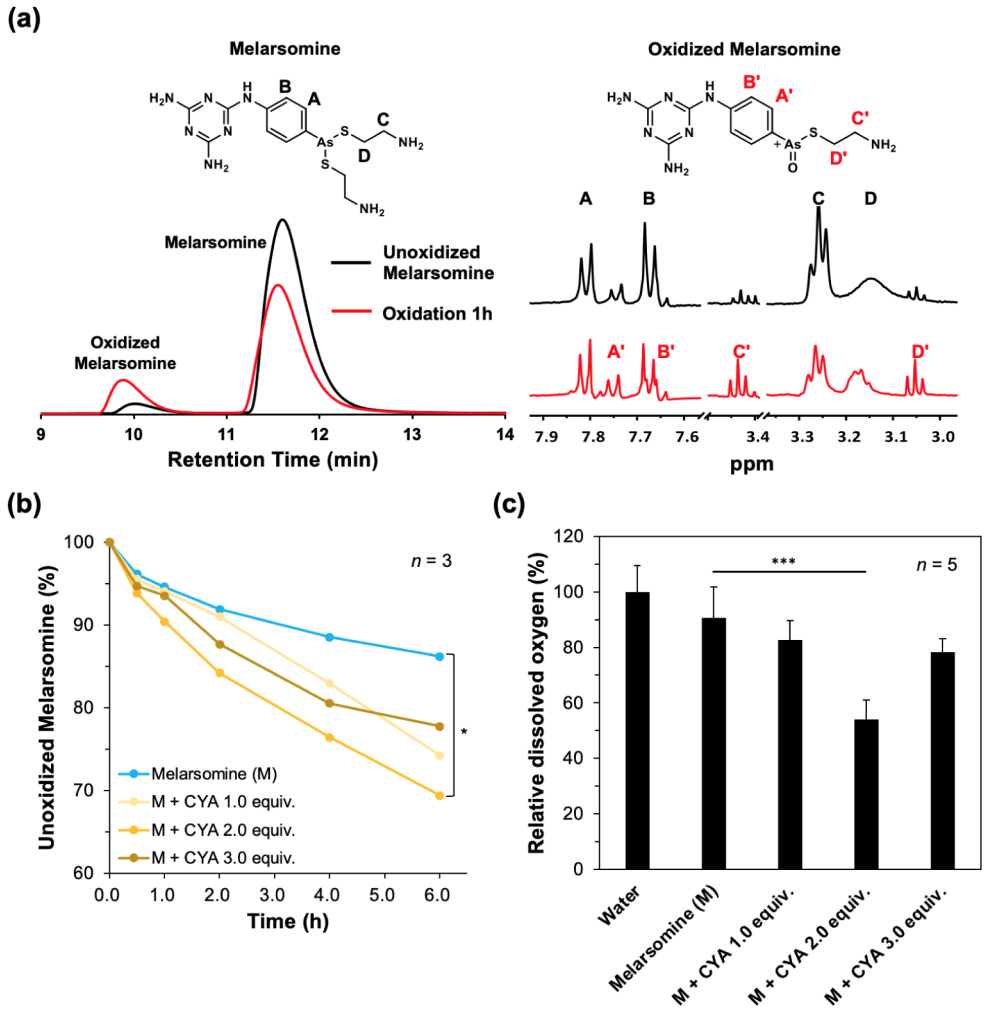

Figure 4. (a) Molecular structures, HPLC results, and ^{1}H NMR spectra of unoxidized and oxidized melarsomine. (b) Percentage of unoxidized melarsomine in supramolecular structures formed by melarsomine and CYA during 6 h of exposure to air. (c) Relative amount of dissolved oxygen in the solution containing the supramolecular structures. *$p < 0.05$; ***$p < 0.001$ ($n = 5$).

conditions was studied using HPLC.[24] In the HPLC chromatogram, the peak observed at 11.5 min corresponded to melarsomine. A small peak was detected at 10 min, which was then analyzed by using mass spectrometry. A mass peak with an M^+ value of 368.1 was observed, which indicated that the bond between arsenic and sulfur was cleaved, and oxygen subsequently bonded to the arsenic atom (Figure S9).[25,26] To confirm that the observed product was formed through oxidation, a small amount of 1% hydrogen peroxide was added to the melarsomine solution. An increase in the peak area at 10 min and a decrease at 11.5 min were observed in the HPLC chromatogram (Figure 4a). ^{1}H NMR spectra revealed an increase in the intensity of peaks A′, B′, C′, and D′ in oxidized melarsomine compared to peaks A, B, C, and D in melarsomine after exposure to oxidation conditions for 1 h (Figures 4a, S10, and S11). Based on these combined results, we can conclude that the peak at 11.5 min in the HPLC chromatogram represents unoxidized melarsomine, while the peak at 10 min represents oxidized melarsomine.

The molecular assembly of compounds can alter their chemical reactivity, leading to different reactions. Our study aimed to investigate whether the supramolecules formed by melarsomine and CYA could modify the oxidation rate of melarsomine. After adding CYA to melarsomine in an aqueous solution, the resulting supramolecular structures were exposed to air with stirring for 0−6 h (Figure S12). The percentage of oxidized melarsomine in the mixture was analyzed using HPLC. After 6 h of exposure to oxygen, only 10% of melarsomine in the sample without CYA was oxidized (Figure 4b). Melarsomine assembled with 2.0 equiv of CYA showed the highest reactivity, with 30% oxidation after 6 h. In contrast, when 1.0 and 3.0 equiv of CYA were added, only 26% and 23% of melarsomine, respectively, underwent oxidation. Therefore, the supramolecular networks formed by 2.0 equiv of CYA and melarsomine were more effective in oxidizing melarsomine than the irregular aggregates (formed using 1.0 equiv of CYA) and sheets (formed using 3.0 equiv of CYA). TEM images revealed that the supramolecular networks maintained their original structure after 6 h of oxidation (Figure S13). To understand the rapid oxidation of melarsomine in its supramolecular network structure, we prepared samples by using an aqueous solution purged with argon gas. Subsequently, the samples were exposed to air and stirred for 30 min. The samples were tested for the quantity of dissolved oxygen not captured by the supramolecular structure by using a dissolved oxygen meter. Interestingly, the amount of dissolved oxygen within the supramolecular networks was only 59% of that in melarsomine alone (Figure 4c). There was a significant difference between the rate of melarsomine

https://doi.org/10.1021/acsomega.4c04247
ACS Omega 2024, 9, 30986−30992

oxidation and that of oxygen captured by the supramolecular network. This indicates that the networks captured dissolved oxygen prior to melarsomine oxidation. To verify that CYA does not affect the concentration of dissolved oxygen, various concentrations of CYA were dissolved in water and aerated for 30 min with continuous stirring. Subsequently, the dissolved oxygen levels in these samples were measured. The results showed that the concentration of dissolved oxygen remained consistent across different CYA levels, demonstrating that CYA did not affect the amount of dissolved oxygen (Figure S14). We then investigated whether adding 2.0 equiv of CYA to melarsomine traps dissolved oxygen within the formed supramolecular networks by examining the effect of network concentration. Samples of supramolecular networks at concentrations of 600 μM, as well as their dilutions to 300 and 150 μM, were exposed to air for 30 min. The dissolved oxygen levels were then measured. As the concentration of the networks decreased, the amount of dissolved oxygen in the samples increased (Figure S15).

To determine whether oxygen captured by the supramolecular networks was more than just a structural phenomenon, we conducted experiments involving the molecular assembly of cyromazine (CYR), a cyclopropyl derivative of melamine, and CYA (Figure S5a). The TEM images used to identify the supramolecular structure of CYR and CYA in aqueous solution revealed that 1.0 equiv of CYA produced loose networks, 2.0 equiv resulted in dense networks, and 3.0 equiv produced very large sheet-like structures (Figure S16a). The structures of the complexes formed between CYR and CYA were comparable to those of the complexes formed between melarsomine and CYA. To assess the oxygen capture capabilities of the supramolecular structures formed using CYR and CYA, we conducted dissolved oxygen measurements. These results indicated that none of the supramolecular complexes composed of CYR and CYA could capture oxygen (Figure S16b). The results of the study showed that supramolecular networks formed by combining 2.0 equiv of CYA with melarsomine capture surrounding oxygen molecules more efficiently than the smaller aggregates formed using 1.0 equiv of CYA and the sheets formed using 3.0 equiv of CYA. The extensive surface area of these 2-D networks allows melarsomine better access to the oxygen trapped in the solution, thereby facilitating oxidation reactions.

3. CONCLUSIONS

We investigated the 2-D supramolecular structures formed by combining melarsomine and CYA through hydrogen bonds. These networks were assembled by varying the concentration of CYA to 1.0, 2.0, and 3.0 equiv relative to melarsomine. Optical microscopy images revealed that 1.0 equiv of CYA and melarsomine formed irregular aggregates, while 2.0 equiv formed networks, and 3.0 equiv produced sheets. Dissolved oxygen measurements demonstrated that the supramolecular network formed by melarsomine with 2.0 equiv of CYA trapped oxygen more effectively than the other structures. This enhanced oxygen capture, facilitated by the large surface area of the network at both the nano- and microscales, was further confirmed by HPLC. This analysis indicated that oxygen absorption by the network promoted the oxidation of melarsomine. This oxidation is crucial, as it exposes arsenic in melarsomine to oxygen, promoting an oxidation reaction. In this study, we utilized CYA to enhance the assembly driven reaction of melarsomine and control its oxidation rate. This study represents a significant initial step toward understanding the mechanisms of melarsomine oxidative degradation.

4. EXPERIMENTAL SECTION

4.1. General Methods. All solvents and organic reagents were obtained from commercial suppliers and used without further purification. Sterile Immiticide powder (melarsomine dihydrochloride) was obtained from Boehringer Ingelheim. Distilled water (DW) was obtained by ion-exchange deionization and filtration. Mass spectrometry was performed using an Expression CMS (Advion) electrospray ionization (ESI) mass spectrometer. Absorption spectra were obtained by using a PerkinElmer Lambda 465 UV−visible spectrophotometer. Fourier transform infrared spectroscopy (FT-IR) was performed by using a Shimadzu IRSpirit instrument in the ATR mode. ^{1}H NMR spectra were obtained on a 400 MHz FT-NMR spectrometer using a JNM-ECZ400S/L1. HPLC was performed using a Shimadzu LC-20AR instrument equipped with a YMC-Triart C18 column (250 × 4.6 mm I.D. S-5 μm). Optical microscopy (OM) images were obtained using a Leica DMi8 fluorescence microscope, and the results were analyzed using the LAS X software (version 3.7.1.21655).

4.2. Preparation of Supramolecular Materials. The DW used to prepare the supramolecular materials was purged with Ar to make them as oxygen-free as possible. Powdered melarsomine (Immiticide) and CYA were dissolved in DW to prepare a stock solution with a concentration of 0.1 wt %. The stock solution was transferred to a sterile vial via a Hamiltonian syringe, and DW was added to achieve the target concentration of the sample. The vials containing the samples were purged with Ar and sealed. The samples were then sonicated for 30 min under ambient conditions. All samples were incubated in the dark in a refrigerator at 4 °C until the supramolecular structures stabilized.

4.3. FT-IR Spectroscopy. The FT-IR spectra of melarsomine and CYA were measured in the ATR mode. The FT-IR spectrum of the sample in which melarsomine (600 μM) and CYA were coassembled was measured after concentrating the sample by repeated drop-casting. The resolutions of all samples were set to eight.

4.4. Molecular Simulations. Molecular simulations were conducted between melarsomine and CYA using the Jaguar module in Schrodinger Maestro software. The B3LYP-D3 functional and the 6-31G** basis set and the Poisson−Boltzmann/Fermi (PBF) water solvent model were employed. The dispersion calculation for B3LYP-D3 in density functional theory (DFT) is a valuable tool for the precise modeling of hydrogen-bond interactions. By including a dispersion correction (D3) to the B3LYP functional, it becomes possible to more accurately capture the weak, noncovalent forces that play a crucial role in hydrogen bonding scenarios. The PBF water solvent model provides a more accurate representation of solvent molecules, particularly water, in simulations. It uses the Poisson−Boltzmann theory to account for electrostatic interactions and the Fermi-like distribution function to simulate the behavior of water molecules around solutes. This approach offers a detailed representation of solvation effects, which is especially useful for studying biomolecular systems.

4.5. Transmission Electron Microscopy. The prepared sample solution (2 μL) was drop-cast onto a carbon-coated grid (Carbon Type B, 12−25 nm thickness, 200 mesh, with Formvar; Ted Pella, Inc.). The solution was then evaporated under ambient conditions and stained by depositing a drop of filtered

https://doi.org/10.1021/acsomega.4c04247
ACS Omega 2024, 9, 30986−30992

uranyl acetate aqueous solution (0.4 wt %) on the surface of the sample-loaded grid. The dried specimen was observed using a Hitachi H-7650 instrument operated at 100 kV in a high-contrast mode.

4.6. Optical Microscopy. Ten microliters of the sample solution was dropped onto a glass slide and covered with a cover glass. The prepared specimens were observed at 100× magnification using an optical microscope.

4.7. HPLC Experiments. First, 20 μL of a sample solution prepared by incubation was injected into the HPLC instrument. The weight of the vial containing the sample was then measured, followed by stirring for a predetermined time. Then, DW was added to the vial until the desired weight was reached before stirring again. Subsequently, the weight of the vial was measured again to maintain the concentration of the sample solution constant. Thereafter, DW was added until the desired weight was reached before stirring. This process was repeated to maintain the concentration of the solution, and the amount of unoxidized melarsomine was analyzed. All samples were analyzed using reverse-phase HPLC. We used a solvent system comprising water/acetonitrile in a 95:5 ratio with a transition to a 0:100 ratio over 30 min. The solvent system contained 0.1% trifluoroacetic acid. A C18 analytical column was used, and quantification was based on the area ratio of the result detected at 254 nm.

4.8. Dissolved Oxygen Measurements. A vial containing the sample solution was opened and stirred for a specific duration. The amount of dissolved oxygen in the sample solution not captured by the supramolecular structures was measured using a dissolved oxygen meter (CAS Dissolved Oxygen TESTER DM-2).

4.9. Statistical Analysis. All tests were conducted in triplicate, and the results were presented as mean ± standard deviation. Student's t test and one-way analysis of variance (ANOVAs) with posthoc Tukey's honest significant difference (HSD) test were used for statistical comparisons between groups. Statistical significance was set at $p < 0.05$.

■ ASSOCIATED CONTENT

Supporting Information

The Supporting Information is available free of charge at https://pubs.acs.org/doi/10.1021/acsomega.4c04247.

TEM image of melarsomine (600 μM) in aqueous solution; absorption coefficients of samples assembled with 600 μM of melarsomine and different equivalents of CYA at 275 nm; ^{1}H NMR spectra of melarsomine with different equivalents of CYA; TEM image of CYA at 600 μM; chemical structure of melamine; ^{1}H NMR spectrum of melamine in D_2O; chemical structure of cyromazine; ^{1}H NMR spectrum of cyromazine in D_2O; DFT calculations of the three hydrogen bond binding modes formed by melarsomine and CYA and their corresponding energy levels; TEM image of CYA (600 μM) in aqueous solution; UV−visible spectra of different concentrations of CYA in water and their absorption coefficients at 214 nm; images of 12 mM of CYA in water; ESI-mass spectrum of oxidized melarsomine; ^{1}H NMR spectrum of melarsomine in D_2O; ^{1}H NMR spectrum of melarsomine oxidized for 1 h in D_2O; percentage of unoxidized melarsomine calculated using HPLC; TEM image of a network structure assembled with melarsomine and 2.0 equiv of CYA after 1 h of oxidation; relative dissolved oxygen content after 30 min of exposure to different concentrations of CYA; relative dissolved oxygen after exposing the supramolecular network samples containing 600 μM, 300 μM, and 150 μM of melarsomine to air for 30 min; TEM images of the structures assembled with different equivalents of CYA added to 600 μM of CYR; amount of dissolved oxygen after 30 min of air exposure of the supramolecular structures formed by adding different amounts of CYA to CYR (PDF)

■ AUTHOR INFORMATION

Corresponding Author

Yongju Kim − *KU-KIST Graduate School of Converging Science and Technology, Korea University, Seoul 02841, Republic of Korea; Department of Integrative Energy Engineering, Korea University, Seoul 02841, Republic of Korea; Chemical and Biological Integrative Research Center, Korea Institute of Science and Technology, Seoul 02792, Republic of Korea;* orcid.org/0000-0002-5862-5228; Email: yongjukim@korea.ac.kr

Authors

Dongjun Baek − *KU-KIST Graduate School of Converging Science and Technology, Korea University, Seoul 02841, Republic of Korea*

Nakyeong Kim − *KU-KIST Graduate School of Converging Science and Technology, Korea University, Seoul 02841, Republic of Korea*

Dahee Jung − *KU-KIST Graduate School of Converging Science and Technology, Korea University, Seoul 02841, Republic of Korea*

Jeong Sook Ha − *Department of Chemical and Biological Engineering, Korea University, Seoul 02841, Republic of Korea;* orcid.org/0000-0003-1358-3295

Complete contact information is available at: https://pubs.acs.org/10.1021/acsomega.4c04247

Author Contributions

#D.B. and N.K. contributed equally to this study.

Notes

The authors declare no competing financial interest.

■ ACKNOWLEDGMENTS

This work was supported by the National Research Foundation of Korea (NRF) grants funded by the Korean government (MSIT) (RS-2024-00352931 and NRF-2022R1A4A1031687), the KIST Institutional Program (2 V10330-24-P042), and a Korea University grant.

■ ABBREVIATIONS

M, melarsomine; CYA, cyanuric acid; CYR, cyromazine; AU, arbitrary unit; FT-IR, Fourier transform infrared; NMR, nuclear magnetic resonance; DFT, density functional theory; TEM, transmission electron microscopy; OM, optical microscopy; 2-D, two-dimensional; DW, distilled water; HPLC, high-performance liquid chromatography

■ REFERENCES

(1) Broer, D. J.; Bastiaansen, C. M.; Debije, M. G.; Schenning, A. P. Functional Organic Materials Based on Polymerized Liquid-Crystal

https://doi.org/10.1021/acsomega.4c04247
ACS Omega 2024, 9, 30986−30992

Monomers: Supramolecular Hydrogen-Bonded Systems. *Angew. Chem., Int. Ed.* **2012**, *51* (29), 7102−7109.
(2) Cheng, P.-N.; Pham, J. D.; Nowick, J. S. The supramolecular chemistry of β-sheets. *J. Am. Chem. Soc.* **2013**, *135* (15), 5477−5492.
(3) Shen, Z.; Jiang, Y.; Wang, T.; Liu, M. Symmetry breaking in the supramolecular gels of an achiral gelator exclusively driven by $\pi-\pi$ stacking. *J. Am. Chem. Soc.* **2015**, *137* (51), 16109−16115.
(4) Xie, Y.; Wang, X.; Huang, R.; Qi, W.; Wang, Y.; Su, R.; He, Z. Electrostatic and aromatic interaction-directed supramolecular self-assembly of a designed Fmoc-tripeptide into helical nanoribbons. *Langmuir* **2015**, *31* (9), 2885−2894.
(5) Zhang, Z.; Lv, Q.; Gao, X.; Chen, L.; Cao, Y.; Yu, S.; He, C.; Chen, X. pH-Responsive poly (ethylene glycol)/poly (L-lactide) supramolecular micelles based on host−guest interaction. *ACS Appl. Mater. Interfaces* **2015**, *7* (16), 8404−8411.
(6) Guo, D.-S.; Wang, K.; Wang, Y.-X.; Liu, Y. Cholinesterase-responsive supramolecular vesicle. *J. Am. Chem. Soc.* **2012**, *134* (24), 10244−10250.
(7) Choi, H.; Cho, K. J.; Seo, H.; Ahn, J.; Liu, J.; Lee, S. S.; Kim, H.; Feng, C.; Jung, J. H. Transfer and dynamic inversion of coassembled supramolecular chirality through 2D-sheet to rolled-up tubular structure. *J. Am. Chem. Soc.* **2017**, *139* (49), 17711−17714.
(8) Vyborna, Y.; Vybornyi, M.; Häner, R. From ribbons to networks: Hierarchical organization of DNA-grafted supramolecular polymers. *J. Am. Chem. Soc.* **2015**, *137* (44), 14051−14054.
(9) Dong, R.; Zhou, Y.; Huang, X.; Zhu, X.; Lu, Y.; Shen, J. Functional supramolecular polymers for biomedical applications. *Adv. Mater.* **2015**, *27* (3), 498−526.
(10) Lv, X. C.; Lu, L.; Zuo, X. X.; Achalkumar, A. S.; Zhao, A. J.; Bermeshev, M. V.; Wang, F. M.; Ngeontae, W.; Ren, X. K. Supramolecular Structure and Photo-Thermo-Electric Property of Hydrogen-Bonded Liquid Crystalline Polymer Containing Poly (4-vinylpridine) and Cyanostilbene Side Chains. *Chem. Eur. J.* **2023**, *29* (20), No. e202204060.
(11) Seo, G.; Jeong, Y.; Kim, Y. Nanostructured Catalytic Reactors Produced by Supramolecular Materials based on Aromatic Amphiphiles. *ACS Mater. Lett.* **2022**, *4*, 1214−1226.
(12) Jiang, Q.; Zhan, W.; Liu, X.; Bai, L.; Wang, M.; Xu, Y.; Liang, G. Assembly drives regioselective azide-alkyne cycloaddition reaction. *Nat. Commun.* **2023**, *14* (1), 3935.
(13) Wang, H.; Wang, Y.; Shen, B.; Liu, X.; Lee, M. Substrate-driven transient self-assembly and spontaneous disassembly directed by chemical reaction with product release. *J. Am. Chem. Soc.* **2019**, *141* (10), 4182−4185.
(14) Liang, H. W.; Guan, Q. F.; Chen, L. F.; Zhu, Z.; Zhang, W. J.; Yu, S. H. Macroscopic-scale template synthesis of robust carbonaceous nanofiber hydrogels and aerogels and their applications. *Angew. Chem., Int. Ed.* **2012**, *51* (21), 5101−5105.
(15) Zhou, M.; Zhang, X.; Bai, M.; Shen, D.; Xu, B.; Kao, J.; Xia, G.; Achilefu, S. Click Reaction-Mediated Functionalization of Near-Infrared Pyrrolopyrrole Cyanine Dyes for Biological Imaging Applications. *RSC Adv.* **2013**, *3* (19), 6756−6758.
(16) Kimizuka, N.; Kawasaki, T.; Hirata, K.; Kunitake, T. Supramolecular Membranes. Spontaneous Assembly of Aqueous Bilayer Membrane via Formation of Hydrogen Bonded Pairs of Melamine and Cyanuric Acid Derivatives. *J. Am. Chem. Soc.* **1998**, *120* (17), 4094−4104.
(17) Mehra, N.; Jeske, M.; Yang, X.; Gu, J.; Kashfipour, M. A.; Li, Y.; Baughman, J. A.; Zhu, J. Hydrogen-bond driven self-assembly of two-dimensional supramolecular melamine-cyanuric acid crystals and its self-alignment in polymer composites for enhanced thermal conduction. *ACS Appl. Polym. Mater.* **2019**, *1* (6), 1291−1300.
(18) Denise, H.; Giroud, C.; Barrett, M. P.; Baltz, T. Affinity chromatography using trypanocidal arsenical drugs identifies a specific interaction between glycerol-3-phosphate dehydrogenase from Trypanosoma brucei and Cymelarsan. *Eur. J. Biochem.* **1999**, *259* (1−2), 339−346.
(19) Narang, A. S.; Desai, D.; Badawy, S. Impact of Excipient Interactions on Solid Dosage Form Stability. *Pharm. Res.* **2012**, *29* (10), 2660−2683.
(20) Perdigão, L. M.; Champness, N. R.; Beton, P. H. Surface self-assembly of the cyanuric acid−melamine hydrogen bonded network. *ChemComm* **2006**, *5*, 538−540.
(21) Chen, Z.; Liu, Y.; Wagner, W.; Stepanenko, V.; Ren, X.; Ogi, S.; Würthner, F. Near-IR absorbing J-aggregate of an amphiphilic BF2-Azadipyrromethene dye by kinetic cooperative self-assembly. *Angew. Chem.* **2017**, *129* (21), 5823−5827.
(22) Disalvo, E. A.; Frias, M. Water state and carbonyl distribution populations in confined regions of lipid bilayers observed by FTIR spectroscopy. *Langmuir* **2013**, *29* (23), 6969−6974.
(23) Song, Y.; Liu, Y.; Qi, T.; Li, G. L. Towards dynamic but supertough healable polymers through biomimetic hierarchical hydrogen-bonding interactions. *Angew. Chem., Int. Ed.* **2018**, *57* (42), 13838−13842.
(24) Gibson, G. G.; Skett, P. *Introduction to drug metabolism*; Springer, 2013.
(25) Berger, B. J.; Fairlamb, A. H. Properties of melarsamine hydrochloride (Cymelarsan) in aqueous solution. *Antimicrob. Agents Chemother.* **1994**, *38* (6), 1298−1302.
(26) Loiseau, P. M.; Lubert, P.; Wolf, J.-G. Contribution of dithiol ligands to in vitro and in vivo trypanocidal activities of dithiaarsanes and investigation of ligand exchange in an aqueous solution. *Antimicrob. Agents Chemother.* **2000**, *44* (11), 2954−2961.

https://doi.org/10.1021/acsomega.4c04247
ACS Omega 2024, 9, 30986−30992